

RESEARCH

Open Access



Targeting NF-kappaB-inducing kinase shapes B-cell homeostasis in myasthenia gravis

Xiaoyu Huang^{1†}, Zhouao Zhang^{1†}, Zhouyi Wang^{1†}, Tiancheng Luo¹, Mingjin Yang¹, Xinyan Guo¹, Xue Du¹, Tianyu Ma¹ and Yong Zhang^{1*}

Abstract

Background B cell immune dysregulation plays a critical role in myasthenia gravis (MG). However, targeted B-cell therapy such as rituximab may result in long-term peripheral B cell clearance and allow for the survival of plasma cells, contributing to frequent infections and relapses. Therefore, we aimed to identify potential novel therapeutic targets that preserve part of B cell function while inhibiting antibody-secreting cells (ASCs).

Methods The transcriptome of sorted CD19⁺B cells obtained from MG patients in active and remission state was performed by RNA sequencing. The hallmark gene NF-kappaB-inducing kinase (NIK/MAP3K14) associated with NF-kB and TNF signaling was identified, and the expression levels of NIK in CD19⁺B cells, CD4⁺T cells and serum from new-onset MG patients and controls were validated by flow cytometry, qPCR and ELISA. In vitro and in vivo, the effects of NIK inhibitor (B022) on the function of CD19⁺B cells and CD4⁺T cells were detected under the MG PBMCs, sorted B cells and experimental autoimmune MG (EAMG) rat model, respectively.

Results The expression levels of NIK were upregulated in CD19⁺B cells, CD4⁺T cells and serum from new-onset MG patients. Notably, increased serum NIK levels were positively correlated with disease severity and decreased with disease remission. NIK inhibitor B022 significantly reduced B-cell activation, proliferation, ASCs differentiation and pathogenic function, as well as CD4⁺T cell activation and Th17 cells differentiation in vitro. Intraperitoneal injection of B022 ameliorated the severity of EAMG rats, and reduced proportion of pathogenic B and T cell subsets, antibody levels and postsynaptic membrane damage.

Conclusions Targeting NIK with small molecule kinase inhibitors can effectively shape B cell homeostasis, and exhibit protective effects in the EAMG rat model, which may be an effective novel treatment strategy for MG.

Keywords Myasthenia gravis, NIK, B cells, Therapeutic targets

Background

Myasthenia gravis (MG) is a prototypical B-cell-mediated autoimmune disease characterised by skeletal muscle fluctuating fatigue and weakness [1]. Peripheral self-tolerance impairment facilitates the differentiation of autoreactive B cells into antibody-secreting cells (ASCs) that produce high-affinity autoantibodies [2]. These autoantibodies bind to the acetylcholine receptor (AChR) itself, or to muscle-specific receptor tyrosine kinase, low-density lipoprotein receptor-related protein 4, and agrin, blocking AChR clustering and leading to postsynaptic membrane transmission dysfunction at

[†]Xiaoyu Huang, Zhouao Zhang and Zhouyi Wang contributed equally to this work.

*Correspondence:

Yong Zhang
zy20037416@163.com

¹ Department of Neurology, Affiliated Hospital of Xuzhou Medical University, No. 99 Huaihai West Road, Quanshan District, Xuzhou, Jiangsu, China



the neuromuscular junction (NMJ), ultimately causing myasthenia [2]. Except for conventional symptomatic and immunosuppressive therapies, the treatment strategies for MG have entered the era of targeted biological agents [3, 4]. B cell depleting therapy (BCDT), specifically rituximab (RTX), an anti-CD20 monoclonal antibody has emerged as effective for the treatment of MG in numerous large uncontrolled trials [5–9]. However, not all patients respond, and some still suffer from relapse after anti-CD20 treatment [10]. This may be explained by the fact that some ASCs (plasmablasts and plasma cells) do not express CD20, thus escaping RTX-mediated depletion and remaining abnormal in the lymph nodes and bone marrow, contributing to relapse [11]. Moreover, RTX results in long-term peripheral B cell depletion, which also increases the risk of infection. Therefore, there is an urgent need to further explore the intrinsic molecular mechanism of pathogenic B cell alterations in MG, which may contribute to the development of novel, more targeted, and reversible therapies.

NF- κ B-inducing kinase (NIK/MAP3K14) is an apical component of TNF receptor superfamily members mediated noncanonical NF- κ B signalling, which has been found to overactive in B cell-mediated autoimmune diseases and B cell malignancies [12–15]. During B cell development, deletion of NIK in adult mice will disrupt B cell responses, including survival, activation, proliferation and differentiation [16]. NIK deficiency also results in reduced germinal center B cells and impairs the ability of B cell class switching [17]. Similar phenotypes have been observed in patients with loss-of-function mutations in NIK that cause multiple aberrations of lymphoid immunity [18]. Together, these data illuminate a critical role for NIK during B cell-mediated immune responses. However, there is no evidence in the literature to clarify the importance and pathological associations between NIK and MG. This prompted us to further explore whether NIK was overexpressed in MG and could serve as a new therapeutic target.

In this study, we investigated the distinct molecular signatures in B cells of MG patients during active and remission phase, particularly focusing on NIK. We further explored the effects of targeting NIK inhibitor B022 on pathogenic cells *in vivo* and *in vitro* (Fig. 1), which may furnish a foundation for the future utilization of NIK inhibitors in the clinical management of MG.

Materials and methods

Subjects

Peripheral anticoagulant whole blood samples from new-onset MG patients ($n=45$) and healthy controls (HCs) ($n=30$), and serum samples from new-onset MG patients ($n=76$) and HCs ($n=50$) were obtained at the

Affiliated Hospital of Xuzhou Medical University. The detailed characteristics of new-onset MG patients and healthy controls (HCs) are summarized in Table 1. Diagnosis of MG was in line with international consensus guidance [19]. The new-onset patients were characterized as first-episode MG patients who had not undergone any form of immunosuppressive therapy, and exclusion criteria as previously described [20]. The cohort of MG patients ($n=4$) in active and remission state included for RNA sequencing, and their characteristics are shown in Table S1. Active MG patients enrolled were new-onset patients in a progressive state. Remission was defined as the patient having no signs or symptoms of MG [19]. Symptoms were assessed primarily using Activities of Daily Living (ADL) and Quantitative Myasthenia Gravis (QMG) scores.

CD19⁺B cell sorting and RNA sequencing

Peripheral blood mononuclear cells (PBMCs) were extracted from fresh anticoagulated blood of MG patients in both active and remission phases using Ficoll gradient centrifugation (Cat#18,061, STEMCELL Technologies). Freshly isolated PBMCs were stained with CD19 MicroBeads and then subjected to positive selection according to the manufacturer's instructions (Cat#130-050-301, Miltenyi). The purity of the isolated B cells was assessed to be >95% by flow cytometry. Sorted B cells were subsequently lysed using TRIzol reagent (Cat#15596018CN, Invitrogen), and the quantity and purity of the extracted RNA were evaluated. RNA-sequencing was performed using the Illumina Novaseq[™] 6000 sequencer (LC-Bio Technology). All bioinformatics were analyzed using the OmicStudio tools (<https://www.omicstudio.cn/tool>).

NIK quantified by flow cytometry

The expression levels of NIK in lymphocyte subsets were detected by FACS Aria III flow cytometer (BD Biosciences). PBMCs were stained for surface markers with anti-CD3-FITC (Cat#317,306), anti-CD19-APC (Cat#302,212), anti-CD4-Percp-Cy5.5 (Cat#300,530), anti-CD8-APC-Cy7 (Cat#344,714) and anti-CD56-APC (Cat#362,504) (all from Biolegend), then fixed and permeabilized using eBioscience[™] Intracellular Fixation & Permeabilization Buffer Set (Cat#88–8824-00, Invitrogen) followed by staining with anti-MAP3K14/NIK-PE (Cat#bs-0074R-PE, Bioss) according to the manufacturer's guidelines.

NIK mRNA quantified by real-time quantitative PCR (RT-qPCR)

Sorted CD19⁺B cells and CD4⁺T cells were reverse transcribed into cDNA by EZ-press Cell to cDNA Kit (Cat#B0003, EZBioscience) according to the

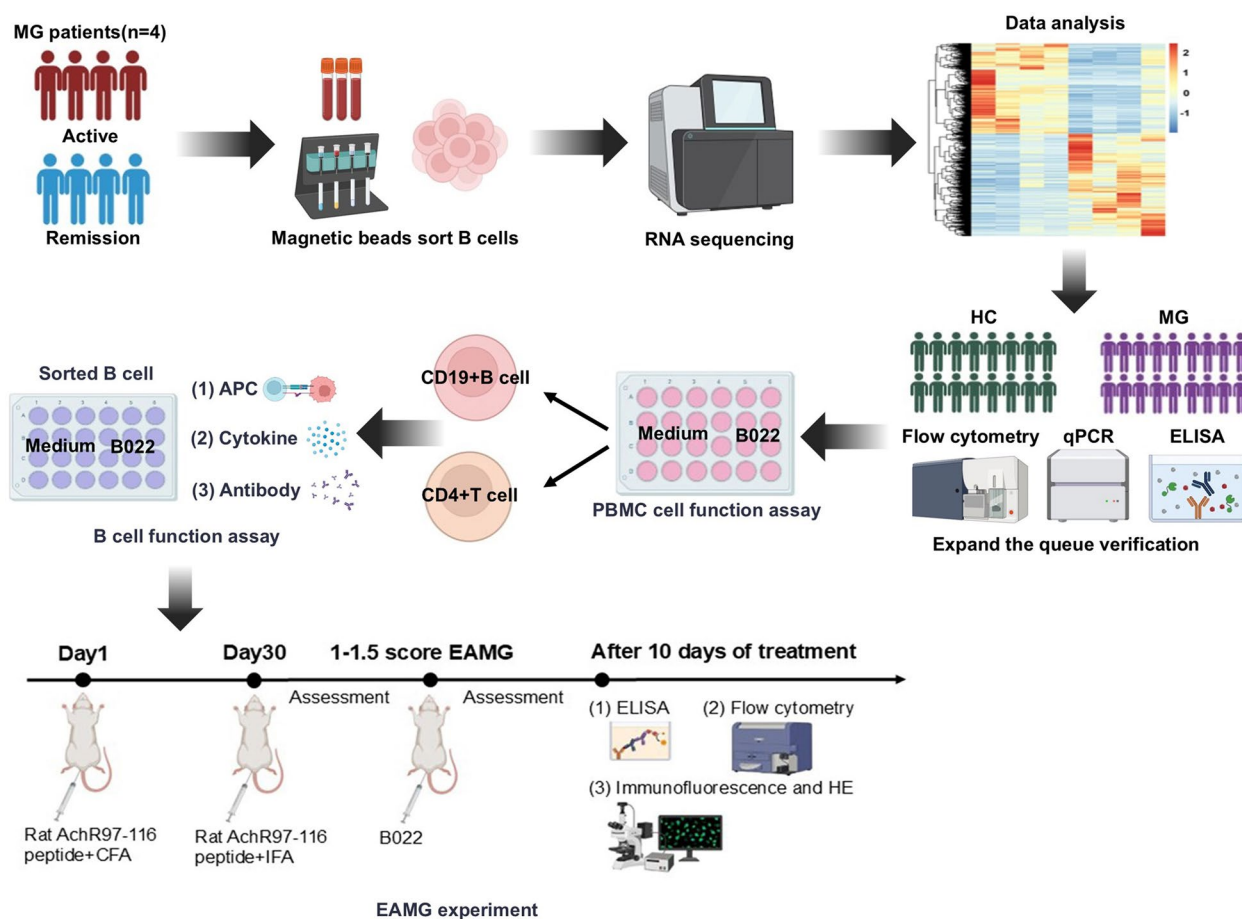


Fig.1 Flowchart of the study

manufacturer’s guidelines. The NIKmRNA expression levels were estimated by RT-qPCR in the Roche LightCycler 480 System using an SYBR Green PCR kit (Cat#A0012, EZBioscience). The relative expression levels of the genes were determined via relative quantification ($2^{-\Delta\Delta CT}$), and the primers used are listed in Table S2.

Enzyme-linked immunosorbent assay (ELISA)

Serum NIK levels were detected with ELISA kits (Cat#MM-62653H1, Jiangsu Meimian Industrial Co.,Ltd) according to the manufacturer’s instructions. Optical densities were recorded at 450 nm, and the concentration was calculated in accordance with the standard curve.

Cell counting kit-8 (CCK-8) assay

Isolated PBMCs were seeded in 96-well plates and treated with NIK inhibitor B022 (0, 50, 100, 200, 500, 1000, 2000, 3000 nmol; Cat#HY-120501, MedChemExpress) for 72 h. Then 10ul CCK8 reagent (Cat#abs50003, Absin Bio science Inc) was added to each well and incubated at 37°C for 4 h. OD values at 450 nm were measured to

plot proliferation curve. The cell viability was calculated according to the manufacturers’ instructions.

Functional PBMCs assay: in vitro activation, survival, proliferation and differentiation

To assess cell activation, survival, proliferation and differentiation, cultured PBMCs stimulated with recombinant human CD40L (50 ng/ml, Cat#310-02-100UG, PeproTech) and F(ab’)2 fragment goat anti-human IgM (10 µg/ml, Cat#109-006-129, Jackson Immuno-research) or CD3 Monoclonal Antibody (OKT3) (2ug/ml, Cat#16-0037-81, eBioscience) and CD28 Monoclonal Antibody (4ug/ml, Cat#14-0289-82, eBioscience) in the presence or absence of NIK inhibitor B022 (1000 nmol) as previously described [21]. After 24 h cultures, B-cell activation markers CD80-FITC (Cat#305,206) and CD86-PE (Cat#374,206) and T-cell activation markers CD25-APC (Cat#385,606) and CD69-PE-Dazzle594 (Cat#310,942) (all from Biolegend) were detected by flow cytometry. After 5-day cultures for B cell and 3-day cultures for T cell, CFSE

Table 1 Characteristics of new onset-MG patients and controls

Characteristics	PBMC for FCM detection			Serum for ELISA detection		
	Controls (n = 32)	New-onset MG(n = 45)	P	Controls (n = 50)	New-onset MG(n = 76)	P
Age, years	57.5(51.00,63.75)	63(48.50,72.00)	0.227	53.00(46.50, 57.25)	55.00(41.25, 65.00)	0.419
Sex, n(%)			0.363			0.207
Female	19(59.38)	22(48.89)		32(64.00)	40(52.63)	
Male	13(40.63)	23(51.11)		18(36.00)	36(47.37)	
Age of onset, n(%)						
EOMG (age < 50 y)		15(33.33)			30(39.47)	
LOMG (age ≥ 50 y)		30(66.67)			46(60.53)	
Type, n(%)						
OMG		20(44.44)			26(34.21)	
GMG		25(55.56)			50(65.79)	
MGFA at admission, n(%)						
I		20(44.44)			26(34.21)	
II		10(22.22)			17(22.37)	
III		11(24.44)			20(26.32)	
IV		4(8.89)			13(17.11)	
Thymoma, n(%)						
Without		34(75.56)			52(68.42)	
With		11(24.44)			24(31.58)	
AchR-Ab, n(%)						
Positive, n(%)		45(100.00)			76(100.00)	
Negative, n(%)		0(0.00)				

Flow cytometry (FCM), Enzyme-linked immunosorbent assay (ELISA), Early-onset myasthenia gravis (EOMG), late-onset myasthenia gravis (LOMG), ocular myasthenia gravis(OMG), generalized myasthenia gravis(GMG), Foundation of America Clinical Classification(MGFA), Acetylcholine receptor antibody (AchR-Ab)

(5µm, Cat# 423,801, Biolegend) labeled cell proliferation assay, Annexin V-FITC (Cat#640,906) and 7AAD (Cat#420,404) labeled apoptosis experiment (Biolegend) were detected by flow cytometry. To assess B and T cell differentiation, cultured cells were stained with a mixture of anti-CD19-APC (Cat#302,212), anti-CD27-BV421 (Cat#356,418), anti-IgD-PE (Cat#348,204), anti-CD38-FITC (Cat#303,504) and anti-CD138-APC-Cy7 (Cat#356,528) (all from Biolegend). For cytokine intracellular staining, cultured PBMCs added 2ul eBioscience™ Cell Stimulation Cocktail (Cat#00-4970-03, Invitrogen) for 5 h. Cells were stained for surface markers with anti-CD3-FITC (Cat#317,306, Biolegend) and anti-CD4-BV421 (Cat#562,424, BD Biosciences), then fixed and permeabilized using eBioscience™ Intracellular Fixation & Permeabilization Buffer Set (Cat#88-8824-00, Invitrogen) followed by staining with anti-IFN-γ-Percp-Cy5.5 (Cat#506,528), anti-IL-4-PE-Cy7 (Cat#500,824) and anti-IL-17A-PE (Cat#512,306) (all from Biolegend). For Treg intracellular staining, cells were stained for surface markers with anti-CD4-FITC (Cat#317,408) and anti-CD25-APC (Cat#385,606) (Biolegend), then fixed and permeabilized using BD Cytotfix/Cytoperm™ reagents (Cat#562,574, BD

Biosciences) followed by staining with anti-FOXP3-PE (Cat#320,208, Biolegend). All samples were analyzed by flow cytometer as described above.

Functional B cell assay: antigen presentation, cytokine and antibody production

Sorted B cells (10^5 /well) were seeded in 96-well plates stimulated with recombinant human CD40L (50 ng/ml, PeproTech), F(ab')₂ fragment goat anti-human IgM (10 µg/ml, Jackson Immunoresearch) and recombinant human IL-21 (50 ng/ml, Cat#8879-IL, R&DSystems) in the presence or absence of NIK inhibitor B022 (1000 nmol) for 5 days. Then, B cells were collected for antibody cocktail staining in response to B-cell antigen presentation (anti-CD19-Percp-Cy5.5 (Cat#302,230), anti-CD80-FITC, anti-CD86-PE, anti-GITR-PE-Cy7 (Cat#371,224), anti-HLA-DR-APC (Cat#307,610) and anti-CD95-BV421 (Cat#305,624)), cytokine production (anti-CD19-APC, anti-IL-6-PE-Cy7 (Cat#501,120), anti-IL-10-PE (Cat#501,404), anti-GM-CSF-Percp-cy5.5 (Cat#502,312) and anti-TNF-α-APC-Cy7(Cat#502,944)) and ASCs differentiation (anti-CD19-APC, anti-CD27-BV421, anti-CD38-FITC and anti-CD138-APC-Cy7) (all from Biolegend) as described above.

Meanwhile, supernatant also was retained for secreted IgG (Cat#V01190H, VICMED) and IgM (Cat#V01200H, VICMED) detection by ELISA kits.

Flow cytometric analysis of NFκB2

For determination of NFκB2-p100/p52 after B022 inhibitor, B cells coated with 50 ng/ml recombinant human CD40L and 10 μg/ml F(ab')₂ fragment goat anti-human IgM were stimulated with 1 μg/ml LPS (Cat#L2630, Sigma-Aldrich) for 30 min in the presence or absence of the 1000 nmol NIK inhibitor B022. Following a 10-min incubation with BD Cytofix Fixation Buffer (Cat#557,870, BD Biosciences) at 37 °C, cells were subsequently permeabilized in BD Phosflow Perm Buffer III (Cat#558,050, BD Biosciences) for 30 min on ice. B cells were stained with Rabbit Anti- NFκB2 antibody (Cat#bs-9418R, Bioss) for 30 min, and then stained with secondary anti-rabbit IgG (H+L)-Alexa Fluor 647 antibody (Cat#4414S, Cell Signaling Technology), followed by flow cytometry analysis.

Transcription factors of B cells differentiated into ASCs by qPCR

Sorted B cells (5×10^5 /well) were seeded in 96-well plates stimulated with CD40L/IgM/IL-21 in the presence or absence of NIK inhibitor B022 for 5 days, then cells were reverse-transcribed into cDNA for qPCR experiments as described above. Primers of transcription factors (IRF4, Blimp-1, XBP-1, ZBTB20, PAX5, BACH2 and IRF8) were listed in Table S2.

In vivo animal experiments

Induction of EAMG and therapeutic experiment

Female Lewis rats (6–8 weeks old) weighing 160–180 g were purchased from Vital River Laboratories (Beijing, China), and bred at the Laboratory Animal Center of Xuzhou Medical University under specific pathogen-free conditions. The rats were provided with standard rat chow and water. The EAMG rat model was induced with rat AChR₉₇₋₁₁₆ peptide (DGDFAIKFKTKVLLDYTGHI) (China Peptides Co. Ltd) following previously reported [22]. Briefly, the rats were immunized subcutaneously at the tail base with a total 200 μl emulsion containing 75 μg of rat AChR₉₇₋₁₁₆ peptide in phosphate buffer saline emulsified in an equal volume of complete Freund's adjuvant containing 1 mg mycobacterium tuberculosis strain H37RA (Cat#231,141, Difco). Then, the rats were boosted on day 30 with the same dose of AChR₉₇₋₁₁₆ peptide in incomplete Freund's adjuvant (Cat#F5506, Sigma-Aldrich). After the second immunization, clinical scores were assessed every day, and then we selected ongoing EAMG rats with onset clinical scores of 1–1.5 for therapeutic experiments. EAMG rats in the B022 group were intraperitoneally given 30 mg/kg B022 for 10 days and

the EAMG model group was injected with an equal volume of cosolvent. The clinical severity score was classified on a scale of 0 to 4, taking into account the presence of tremors, hunched posture, muscle strength, and fatigability as previously outlined [22].

Serum anti-AChR₉₇₋₁₁₆ peptide antibody detection

Rat serum anti-AChR₉₇₋₁₁₆ IgG (Cat#405,428), IgG1 (Cat#407,403), IgG2a (Cat#407,503) and IgG2b (Cat#408,203) (Biolegend) antibody levels were detected by ELISA as previously described [22]. Optical densities were measured at 450 nm.

Hematoxylin–eosin (HE) staining

Paraffin-embedded sections of the spleen, lymph node and muscle from the two groups were stained using an HE staining kit (Cat#G1076-500ML, Service bio) according to the manufacturer's instructions. Subsequent to the application of neutral gum to the slices, the slides were sealed, and the sections were observed under a microscope.

Histological immunofluorescence

To visualize AChR clusters and complement deposition in the postsynaptic membranes of neuromuscular junctions in the tibialis anterior muscles of two groups, a histological immunofluorescence technique was employed. The slides (10 μm) were permitted to air dry before being fixed with cold acetone. After being washed with PBS, the sections were blocked by 4% BSA for 120 min at room temperature and then subjected to an overnight incubation at 4 °C with a mouse anti-rat C5b-9 antibody (1:100, Cat#sc-66190, Santa Cruz). Following another wash, the sections were treated with Alexa Fluor594-conjugated anti-mouse IgG (1:500, Cat#ab150116, Abcam) and CF488-conjugated α-BTX (1:500, Cat#00005, Biotium) for 60 min. Eventually, after a final wash, the sections were inspected under the fluorescence microscope.

Effect of B022 on pathogenic immune cell subsets by flow cytometry

After 10 days of treatment, MNCs isolated from blood, spleen and lymph nodes of two groups were collected and labeled with various antibody combinations. Surface staining, Th membrane staining, and Treg intracellular staining methods refer to the steps above. Flow cytometric analysis was performed using the following fluorescently labeled anti-rat antibodies: anti-CD4-APC-Cy7 (Cat#201,518), anti-CD25-PE (Cat#202,105), anti-CD45RA-FITC (Cat#202,305), anti-CD27-APC (Cat#124,212), anti-CD38-PE (Cat#250,505) (all from Biolegend), anti-CD3-BV421 (Cat#563,948, BD Biosciences), anti-B220-PE-Cy7 (Cat#25-0460-82),

anti-IL-17A-APC (Cat#17-7177-81), anti-FOXP3-Percp-cy5.5 (Cat#45-5773-82) (all from Invitrogen), and anti-PNA Fluorescein (Cat#FL-1071, Vector laboratory).

Statistical analysis

The data are presented as mean \pm standard deviation or median with interquartile ranges. Categorical variables were evaluated using chi-square tests. For data following a normal distribution, an independent-samples t-test was employed, whereas the Mann–Whitney U test was utilized for skewed data. In the case of three or more data sets, means were compared with one-way ANOVA. To investigate the relationship between variables, Spearman's correlation analysis was conducted. Receiver operating characteristic (ROC) curve analysis was conducted to evaluate the predictive value of NIK for MG. All statistical analyses were performed using GraphPad Prism 8.0 (GraphPad Software, La Jolla, CA, USA). Statistical significance was set at a p-value of less than 0.05.

Results

Altered NF- κ B and TNF associated gene expression signature in B cells of MG patients during active and remission phase

RNA sequencing was performed on sorted peripheral B cells, obtained from 4 patients with MG during active and remission phase (Fig. 2A). The thresholds for the up- and downregulated genes were fold change >1.5 or fold change <0.67 and P value <0.05 , and we identified 4591 differentially expressed genes (Table S3). Then, we carried out a comprehensive Gene Set Enrichment Analysis (GSEA) utilizing the extensive collection of gene sets available in MSigDB. Among these, our primary attention was directed towards the hallmark sets, aiming to pinpoint distinct molecular signatures that exhibit differential expression patterns in B cells derived from patients with active MG, as opposed to those from patients in remission. We found that gene sets associated with NF- κ B and TNF signaling were upregulated in B cells from MG patients during active phase (FDR value = 0.032, FDR value = 0.033, Fig. 2B). Moreover, we intersected the differentially expressed genes with those in the NF- κ B (8433 genes, Table S3) and TNF signaling pathways (266 genes, Table S3) in the Genecard database and found 39 differentially expressed genes (Fig. 2C). The expression of MAP3K14 (NIK), a crucial mediator regulating B-cell development and function, was up-regulated in B cells of MG patients in active stage (fold change = 1.783, p-value = 0.013, Fig. 2D). Together, these data indicate that NIK/MAP3K14, a hallmark gene associated with the NF- κ B and TNF signaling, was upregulated in B cells of MG patients with active disease compared to disease remission.

NIK is upregulated in B cells and CD4⁺T cells from patients with MG

We detected NIK expression on lymphocyte subsets by flow cytometry and found that NIK expression was elevated on B cells and CD4⁺T cells in newly diagnosed MG patients compared with HCs ($P < 0.05$, Fig. 2E, H), but no significant difference in NK cells and CD8⁺T cells ($P > 0.05$, Fig. 2G, I). Further, we used qPCR technology to detect NIK mRNA levels, and also found that NIK expression increased in B cells and CD4⁺T cells of MG patients ($P < 0.05$, Fig. 2J, K). These data suggest that NIK expression is up-regulated in pathogenic immune cells of MG patients, which may be involved in the pathogenesis of MG.

Correlations of serum NIK levels with different disease subtypes, clinical severity score, B cell subsets and disease status in MG patients

Serum NIK levels were higher in new-onset MG patients compared with HCs ($P < 0.05$, Fig. 3A). Subgroup analysis revealed that NIK levels were increased in GMG patients than in OMG ($P < 0.01$, Fig. 3D), as well as elevated in thymoma associated MG (TAMG) than in non-TAMG ($P < 0.05$, Fig. 3E). However, no difference was observed between male and female ($P > 0.05$, Fig. 3B), early-onset MG (EOMG) and late-onset MG (LOMG) ($P > 0.05$, Fig. 3C). A correlation heat map was constructed (Fig. 3F), showing that NIK levels were positively correlated with QMG score, MGFA classification and Memory B cells ($r_s = 0.535$, $P < 0.001$; $r_s = 0.422$, $P < 0.001$; $r_s = 0.519$, $P < 0.001$; Fig. 3G–I), but the correlation between serum NIK levels and plasmablast cells was weak despite being statistically significant ($r_s = 0.244$, $P < 0.05$, Fig. 3J). Moreover, we conducted an in-depth longitudinal analysis to scrutinize the dynamics of serum NIK levels and the composition of B cell subsets in a cohort of 22 MG patients. By meticulously comparing these biomarkers during the acute onset and remission phases of the disease, we uncovered a compelling trend: as the MG symptoms waned and the patients transitioned into a state of remission, there emerged a statistically significant decline in both the serum NIK concentrations and the percentages of memory B cells, plasmablasts, and plasma cells ($P < 0.05$, Fig. 3K–N). Univariate ROC curve analysis was performed to evaluate the diagnostic significance of NIK in MG. The findings indicated that the area under the curve (AUC) for NIK was 0.621 ($P < 0.05$, Fig. 3O). These findings demonstrate that serum NIK expression levels correlate with disease severity and disease status, and may be a novel biomarker.

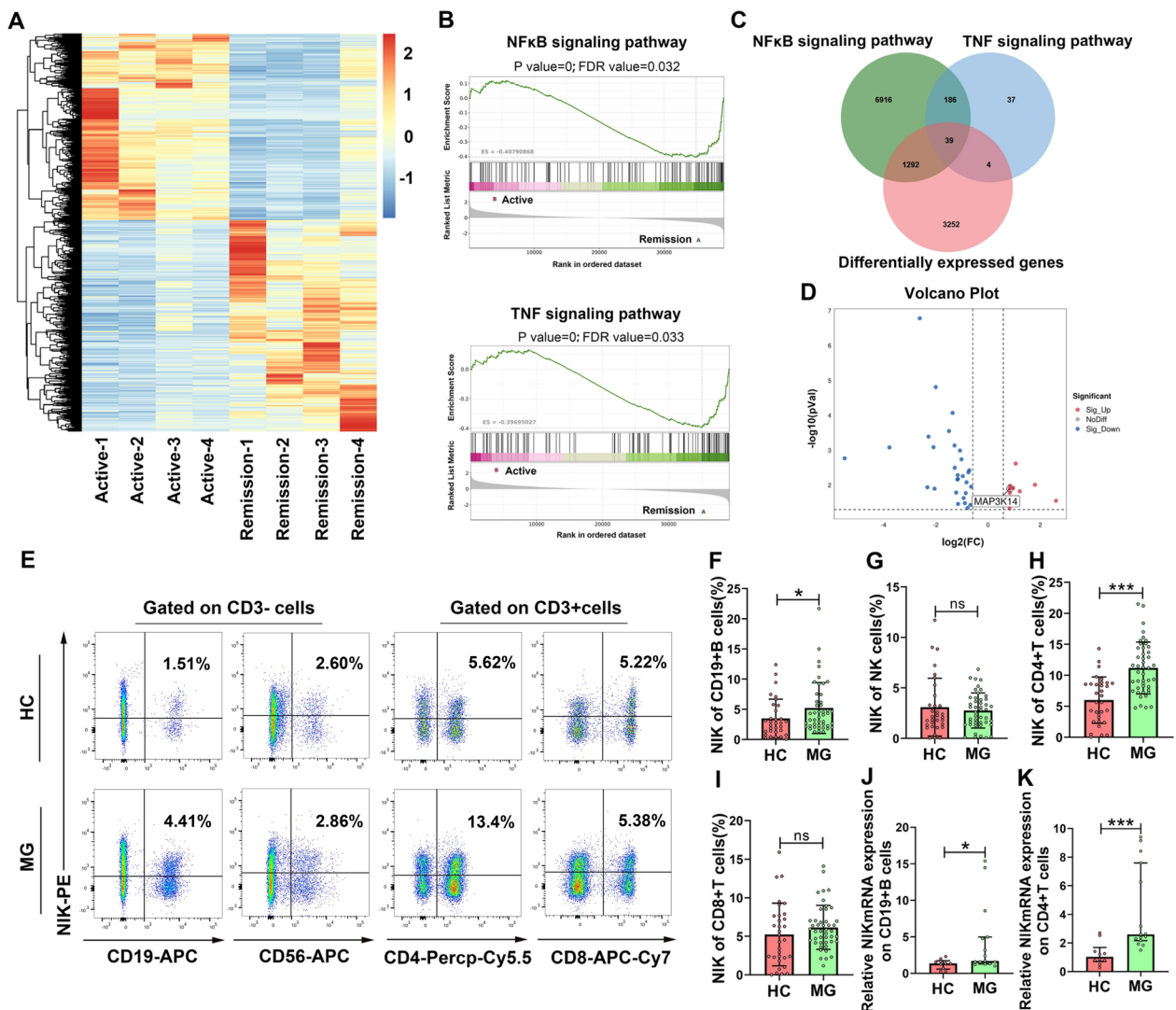


Fig.2 NIK is upregulated in B cells and CD4⁺T cells from MG patients. **A** RNAseq analysis of CD19⁺B cells from MG patients (n=4) during active and remission phase. **B** Gene Set Enrichment Analysis (GSEA) utilizing all gene sets from MSigDB, where gene sets associated with NF-κB and TNF signaling were significantly upregulated. **C** RNAseq differential genes intersect with NF-κB and TNF signaling pathway genes in Genecard database. **D** Volcano plots for 39 differentially expressed genes. Red dots represent up-regulated differential genes (fold change > 1.5, P value < 0.05), blue dots represent down-regulated differential genes (fold change < 0.67, P < 0.05), and non-significant differential genes are shown in gray. **E–I** NIK expression on lymphocyte subsets between HCs (n = 32) and new-onset MG patients (n = 45) detected by flow cytometry. **J–K** NIKmRNA levels on B cells and CD4⁺T cells between HCs (n = 10) and new-onset MG patients (n = 15) detected by qPCR. Data are displayed as means ± SD or median with interquartile ranges. Statistical analysis was conducted by independent sample t-test (normal distribution) or Mann–Whitney U test (non-normal distribution) (*P < 0.05, **P < 0.01, ***P < 0.001, ns: non-significant)

NIK inhibitor B022 attenuates B cell activation, proliferation and differentiation, but has no significant effects on cell apoptosis

To assess the effect of NIK inhibitor B022 on PBMCs viability, we performed CCK-8 assays to determine cell viability under different concentrations of B022. The results showed that B022 suppressed the cell proliferation in a dose-dependent manner and the optimal dose of B022 was 1000 nmol (Fig. 4A). PBMCs from

9 new-onset MG were exposed to 1000 nmol B022 to examine the effect of NIK on lymphocyte subsets and B cell development. The results showed that the percentage of CD19⁺B cells in the B022 inhibitor group was lower than that in the medium group (P < 0.05, Fig. 4B), but the proportions of CD4⁺T cells, CD8⁺T cells, and NK cells had no effect (P > 0.05, Fig. 4B). We also discovered that B022 suppressed the expression of B cell activation markers CD80 and CD86, the

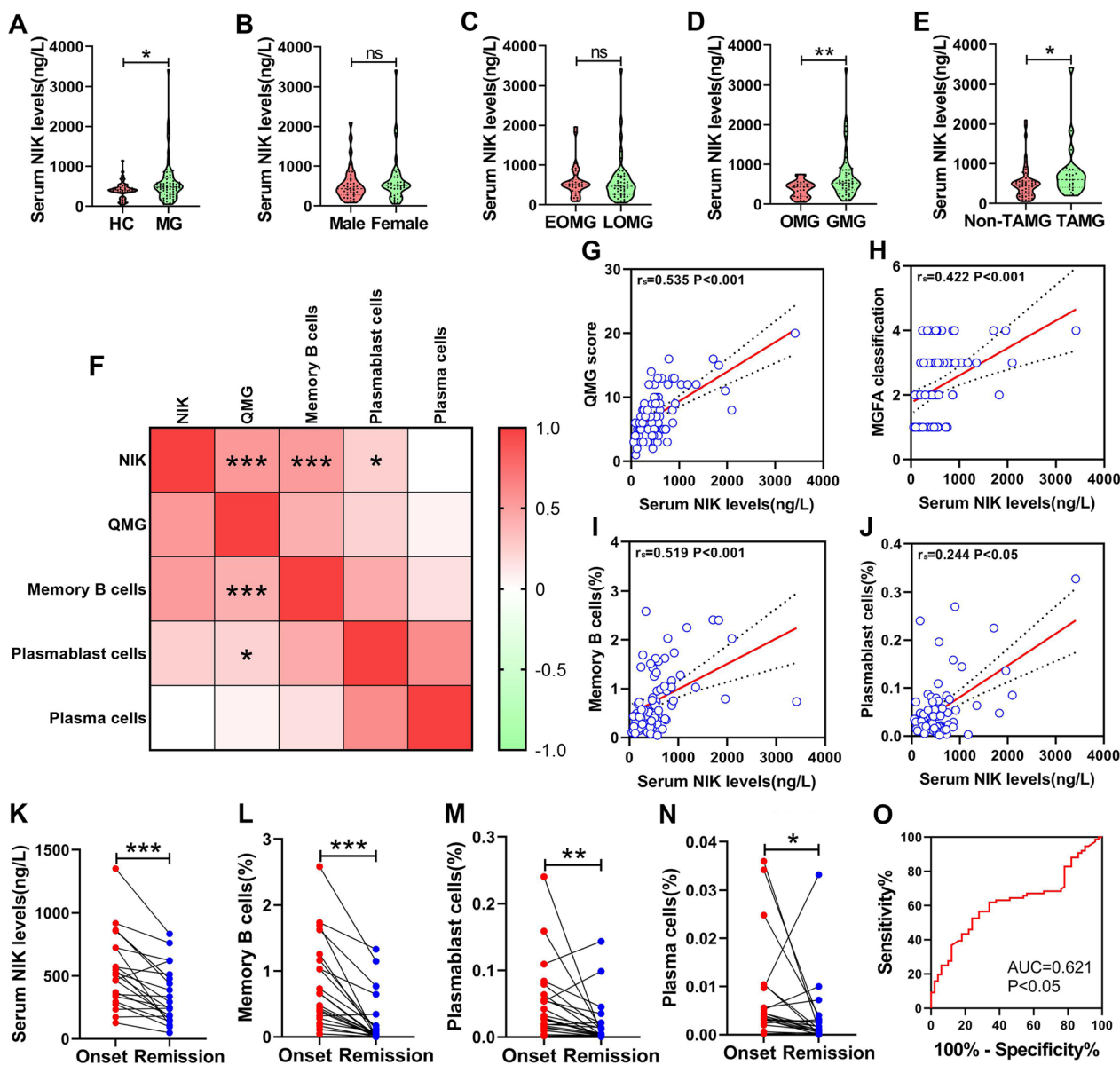


Fig.3 Correlations of serum NIK levels with different disease subtypes, clinical severity score, B cell subsets and disease status in MG patients. **A–E** Serum NIK levels between HCs (n = 50) and new-onset MG (n = 76), male MG (n = 36) and female MG (n = 40), EOMG (n = 30) and LOMG (n = 46), OMG (n = 26) and GMG (n = 50), and non-TAMG (n = 52) and TAMG (n = 24). Data are displayed as means ± SD or median with interquartile ranges. Statistical analysis was conducted by independent sample t-test (normal distribution) or Mann–Whitney U test (non-normal distribution) (*P < 0.05, **P < 0.01, ***P < 0.001, ns: non-significant). **F** Heat map displaying correlations of NIK levels with clinical severity of MG patients and B cell subsets. **G–J** NIK levels were positively correlated with QMG score, MGFA classification and plasmablast cells. Statistical analysis was conducted by spearman’s correlation analysis. **K–N** Serum NIK levels during the acute onset and remission phases of MG patients (n = 22). Data are displayed as means ± SD. Statistical analysis was conducted by Paired sample t test (*P < 0.05, **P < 0.01, ***P < 0.001, ns: non-significant). **O** ROC for diagnostic value of NIK in MG

proliferation of B cells, as well as the formation of switched memory B cells and plasmablasts (P < 0.05, Fig. 4C, F, H, K). Compared with the medium group, the apoptosis rate of B cells and other B cell subsets in the B022 group had no significant difference (P > 0.05, Fig. 4E, I, J, L). These findings demonstrate

that 1000 nmol B022 do not have toxic effects on cell viability and apoptosis of PBMCs, but can modulate B cell activation, proliferation and plasmablasts differentiation in vitro.

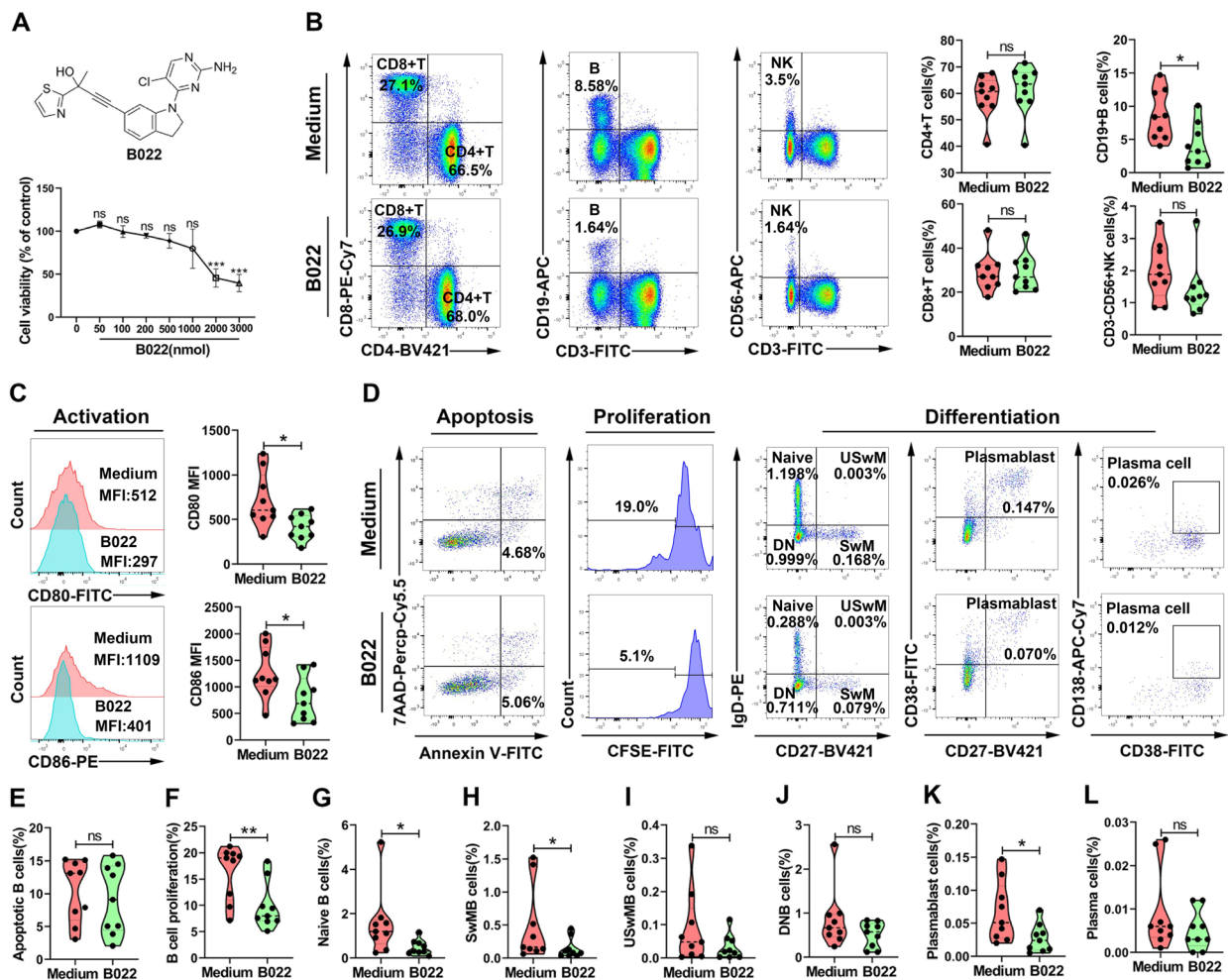


Fig.4 Effect of NIK inhibitor B022 on B cell activation, survival, proliferation and differentiation under MG PBMCs culture system in vitro. **A** CCK-8 assay determined the cell viability under the different concentrations of B022 (n = 3). **B** The percentage of lymphocyte subsets (CD4⁺T, CD8⁺T, CD19⁺B and NK cell) between medium and B022 group (n = 9). **C** Mean fluorescence intensity (MFI) of CD80 and CD86 between medium and B022 group (n = 9). **D–L** The percentage of B cell apoptosis rate, proliferation and B cell subsets (naive B, switched memory B (SwMB), unswitched memory B (USwMB), double negative B (DNB), plasmablast cell and plasma cell) between medium and B022 group (n = 9). Data are displayed as means ± SD. Statistical analysis was conducted by independent sample t-test (*P < 0.05, **P < 0.01, ***P < 0.001, ns: non-significant)

NIK inhibitor B022 attenuates CD4⁺T cell activation and differentiation, but has no significant effects on cell apoptosis and proliferation

To investigate whether the targeting of NIK influenced T cell responses, PBMCs from 9 new-onset MG were cultured in our experimental system with the addition of specific inhibitors. The results showed that B022 suppressed the expression of CD4⁺T cell activation markers CD25 and CD69, and the formation of Th1, Th17 and Treg cells (P < 0.05, Fig. 5B, C, F–I). Compared with the medium group, the apoptosis rate and proliferation of CD4⁺T and the percentage of Th2 cells in the B022 group had no significant difference (P > 0.05, Fig. 5D, E, G). These data indicate that CD4⁺T cell activation

and differentiation can similarly be reversed by the NIK inhibitor B022.

NIK inhibitor B022 effectively attenuates essential B cell pathogenic functions, transcriptional regulators for plasma cell differentiation and NFκB2 pathway

We established *in vitro* B cell culture conditions to investigate the effects of B022 on the B cell functional roles of the antigen presentation, cytokine secretion and antibody production. The results showed that B022 significantly inhibited the expression of costimulatory molecules CD80, CD86 and CD95, inflammatory cytokines IL-6 and GM-CSF, as well as plasmablasts and plasma cells formation (P < 0.05, Fig. 6A–F), but GITR, HLA-DR,

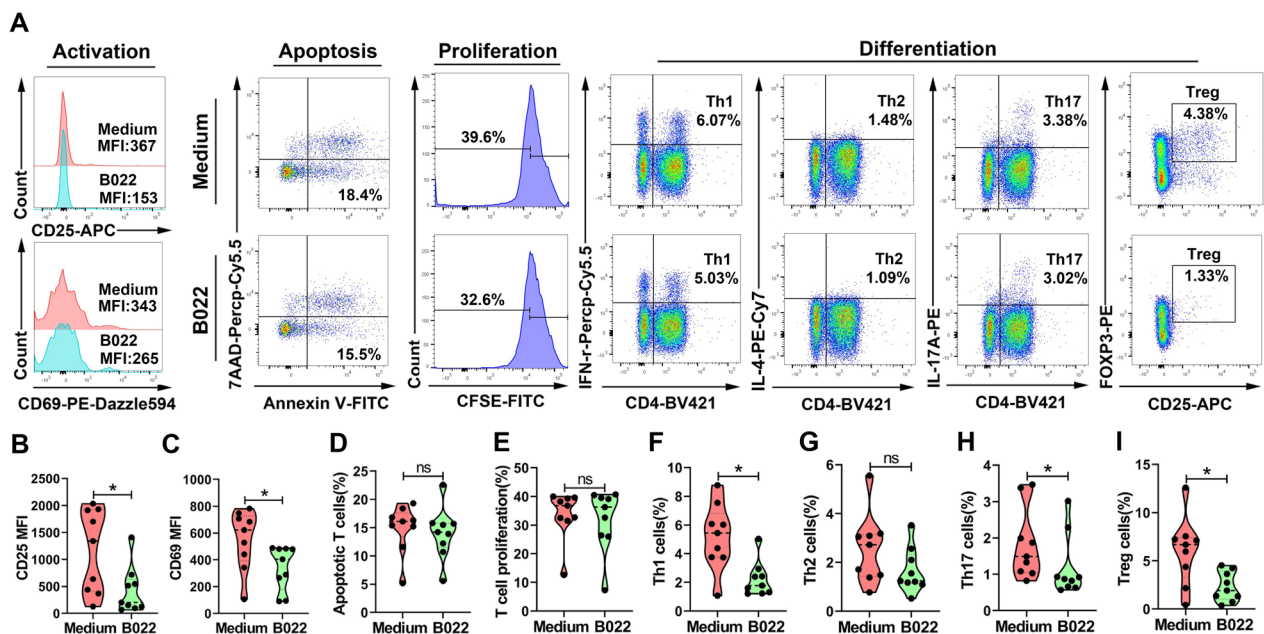


Fig.5 Effect of NIK inhibitor B022 on CD4⁺T cell activation, survival, proliferation and differentiation under MG PBMCs culture system in vitro. **A** The dot plots or peak plots represent flow gating diagram of CD4⁺T cell activation, apoptosis, proliferation and CD4⁺T cell subsets (Th1, Th2, Th17 and Treg). **B–I** The expression of CD4⁺T cell activation markers CD25 and CD69, apoptosis rate, proliferation and T cell subsets between medium and B022 group (n=9). Data are displayed as means ± SD. Statistical analysis was conducted by independent sample t-test (*P < 0.05, **P < 0.01, ***P < 0.001, ns: non-significant)

IL-10 and TNF- α were not influenced ($P > 0.05$, Fig. 6A–D). In line with the effects observed on antibody secreting cells (ASCs) differentiation, B022 significantly inhibited the production of IgM and IgG ($P < 0.05$, Fig. 6I, J). We also probed whether the expression of plasma cell transcriptional regulators was affected. qPCR revealed that the expression of IRF4, Blimp-1 and XBP-1 was significantly decreased, while the expression of PAX5, BACH2 and IRF8 was increased in the presence of NIK inhibitors ($P < 0.05$, Fig. 6K). At the same time, the inhibitory effect of B022 on NIK-mediated NF κ B2 activation was observed ($P < 0.05$, Fig. 6G, H). Altogether, these findings indicate that NIK inhibitor B022 may affect B-cell antigen presentation, cytokine production and antibody production by inhibiting NF κ B2 pathway, which is consistent with the observation of PBMC culture system, and once again indicates the important regulatory role of NIK on the homeostasis of B cells.

B022 alleviated clinical manifestations, decreased serum antibody levels, and improved the morphological changes and complement deposition at NMJ in EAMG rats

After two immunizations, we randomly selected 10 ongoing EAMG rats with onset clinical scores of 1–1.5 for therapeutic experiments. Five EAMG rats in the B022 group were intraperitoneally given 30 mg/kg B022 for 10 days and 5 EAMG rats in the EAMG model group

were injected with an equal volume of cosolvent. When compared to the EAMG group, EAMG rats treated with B022 showed a significant reduction in weight loss and exhibited markedly lower clinical scores ($P < 0.05$, Fig. 7D, E). Additionally, the concentrations of anti-AChR₉₇₋₁₁₆ IgG, IgG2a, and IgG2b in the serum of the B022-treated EAMG rats were substantially lower than those in the EAMG group ($P < 0.05$, Fig. 7F–I). After treatment with B022, the morphological changes of spleen, lymph node and muscle tissues of rats were investigated. Compared with EAMG rats, the size of splenic nodules and lymphatic nodules decreased or atrophied, and the disorganized rupture and tightness of skeletal muscle fibers were improved to some extent, and the inflammatory infiltration were gradually reduced in the B022 treatment group (Fig. 7J). To gain deeper insights into the structure of AChR and complement deposition within the postsynaptic membranes of rat NMJ, we utilized tissue immunofluorescence techniques for detailed observation of NMJ structure. Our findings revealed a notable increase in the number of AChR clusters and a concurrent reduction in complement deposition following B022 treatment. (Fig. 7K). Besides, we also detected the expression of NIKmRNA in spleen tissues of HC, EAMG and B022 groups, and found that the expression level of NIKmRNA in EAMG rats was higher than that in HC rats ($P < 0.001$, Fig. S7). Compared with EAMG rats, NIKmRNA

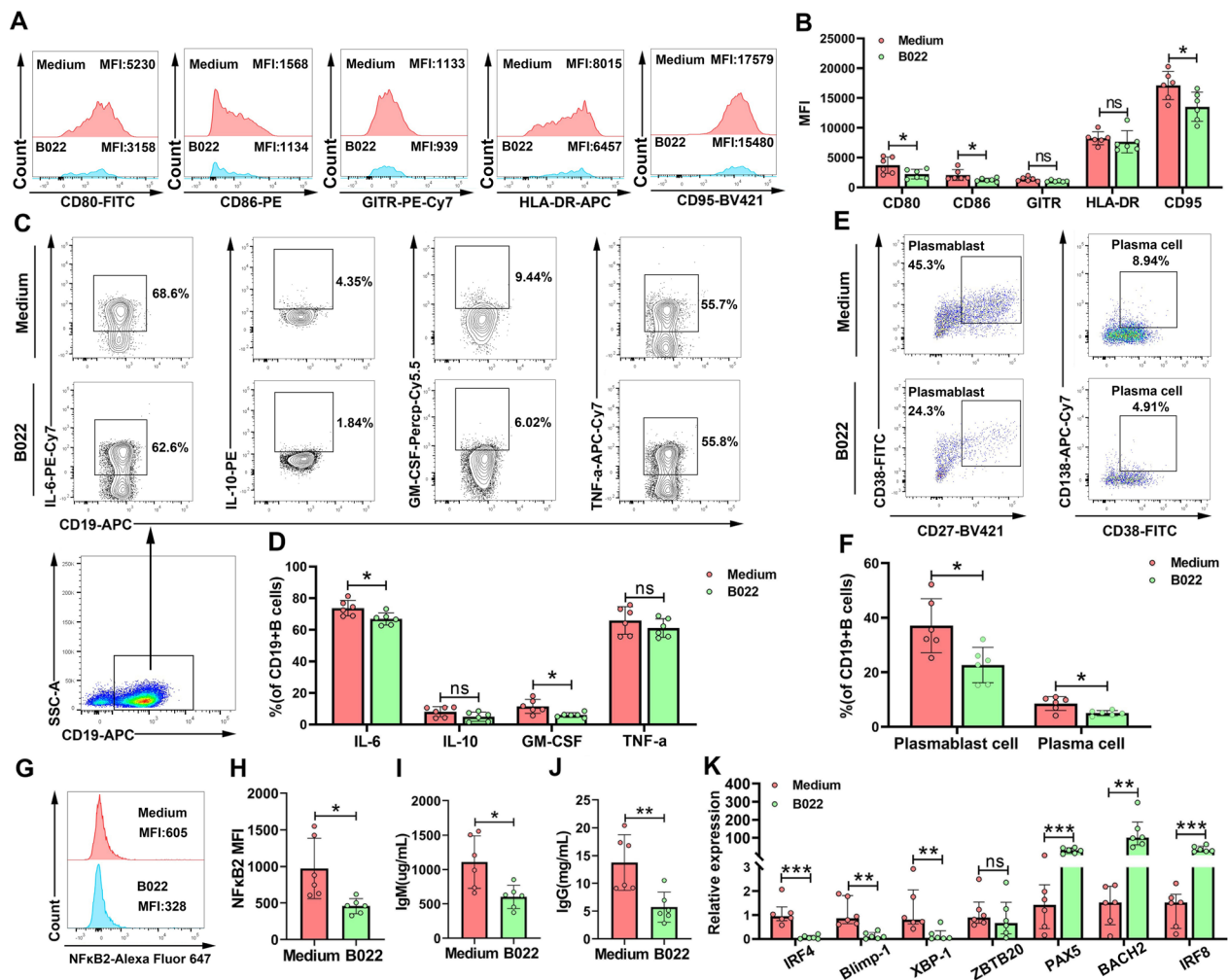


Fig.6 Effect of NIK inhibitor B022 on B cell function under MG sorted B cell culture system in vitro. **A** The peak plots represent flow gating diagram of B cell antigen presenting marker (CD80, CD86, GITR, HLA-DR and CD95). **B** MFI of CD80, CD86, GITR, HLA-DR and CD95 between medium and B022 group (n=6). **C** The contour plots represent flow gating diagram of B cell associated cytokines (IL-6, IL-10, GM-CSF and TNF-α). **D** The percentage of IL-6, IL-10, GM-CSF and TNF-α between medium and B022 group (n=6). **E** The dot plots represent flow gating diagram of plasmablast and plasma cells. **F** The percentage of plasmablast and plasma cells between medium and B022 group (n=6). **G** The peak plots represent flow gating diagram of NfκB2. **H** MFI of NfκB2 between medium and B022 group (n=6). **I–J** Titers of IgM and IgG from cultured supernatant between medium and B022 group (n=6). **K** Relative expression of plasma cell related transcription factors (IRF4, Blimp-1, XBP-1, ZBTB20, PAX5, BACH2 and IRF8) between medium and B022 group (n=6). Data are displayed as means ± SD. Statistical analysis was conducted by independent sample t-test (*P < 0.05, **P < 0.01, ***P < 0.001, ns: non-significant)

expression decreased after B022 treatment (P < 0.001, Fig. S7), suggesting that NIK also plays an important role in EAMG rat models. These data position NIK inhibition in vivo leads to reduced disease severity, decreased pathogenic antibody titers, and improved neuromuscular junction lesion structure.

B022 alters the frequency of EAMG rat B and CD4⁺T cell subsets in vivo

In order to further elucidate the therapeutic potential of B022 inhibitors from the immunomodulatory

mechanisms in vivo, we also evaluated the changes of CD4⁺T and B cell subsets in peripheral blood, lymph nodes, and spleen of EAMG rats after B022 treatment. We found that NIK inhibitor B022 down-regulated the frequency of total B cells, memory B cells, germinal center B, ASCs and Th17 cells (P < 0.05, Fig. 8), but there was no significant effect on the percentage of Treg cells (P > 0.05, Fig. 8). Together, the in vivo data also observe that NIK inhibitor leads to downregulation of pathogenic immune cells in EAMG rats, and NIK may be an important therapeutic target.

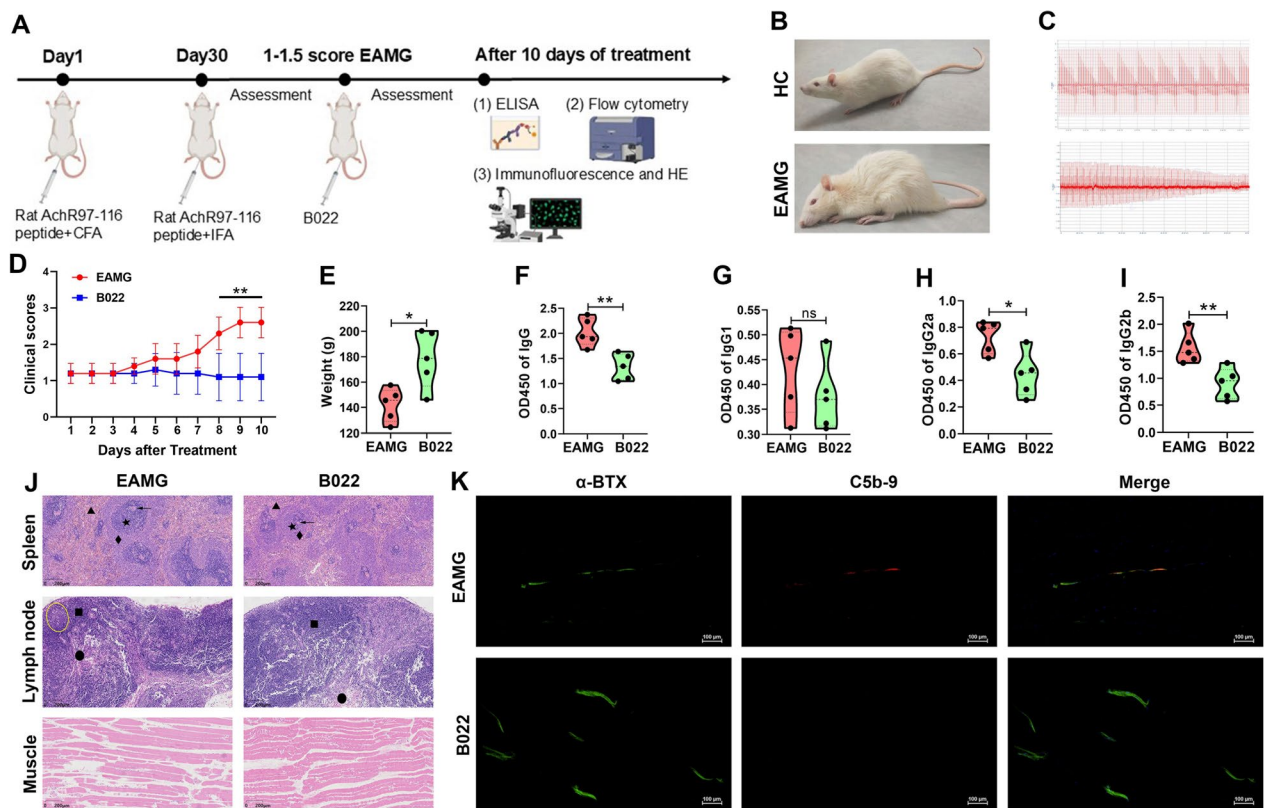


Fig.7 B022 alleviated clinical symptoms, reduced serum antibody levels, and improved the morphological changes and complement deposition at NMJ in EAMG rats. **A** Flow chart of animal experiment. **B** HC and EAMG rat model picture. **C** Electrophysiology of healthy and EAMG rats. **D** The clinical scores of EAMG and B022 treated rats were recorded every day after treatment (n = 5). **E** The weights of EAMG and B022 treated rats on the last day (n = 5). **F–I** Serum AChR₉₇₋₁₁₆ IgG, IgG1, IgG2a and IgG2b levels from these two groups were detected by ELISA (n = 5). **J** The morphological changes of spleen, lymph nodes and muscle were observed after B022 treatment. Arrow represents central artery; Five-pointed star represents splenic nodules; Diamond represents marginal area; Triangle represents red marrow; Square represents cortex; Circle represents medulla; Yellow circle represents lymph nodules. **K** Immunofluorescence of neuromuscular junction structure AChR clusters (green) and complement deposition C5b-9 (red). Data are displayed as means ± SD. Statistical analysis was conducted by independent sample t-test (*P < 0.05, **P < 0.01, ***P < 0.001, ns: non-significant)

Discussion

MG is a typical B-cell-mediated autoimmune disorder, and achieving sustained remission is of crucial significance for enhancing patients' quality of life. The differentiation of B cells into plasma cells to produce pathogenic antibodies is the core immunological event leading to the pathogenesis of MG [23]. Given the important roles of B cells, targeted B-cell therapy is increasingly being used in the clinic and has shown certain benefits [24]. However, rituximab or ocrelizumab, B cell-depleting therapy targeting CD20 molecules, may completely disrupt the humoral immune response and increase the risk of infection [24]. Therefore, a comprehensive exploration of the B cell features in MG patients during the remission phase is of paramount importance for identifying novel therapeutic targets aimed at B cells. In the current study, we found that NIK/MAP3K14, a hallmark gene associated with NF-κB and TNF signaling, was upregulated in

B cells of MG patients with active disease compared to those in remission. On this premise, we evaluated the immunomodulatory effects of NIK inhibitor B022 on pathogenic cells *in vitro* and *in vivo*, and observed that B022 effectively attenuates B cell development and function, which may provide an effective novel treatment strategy for MG.

NIK is a crucial signaling component within the non-canonical NF-κB pathway, which integrates signals from a subset of TNF receptor family members and activates a downstream kinase, IκB kinase-α, thereby triggering p100 phosphorylation and processing [25]. Cumulative evidence demonstrates that NIK participates in numerous indispensable cellular processes and is pivotal for the function and development of B and T cells, which plays an important role in the regulation of immunity and inflammation [26, 27]. NIK deficiency is associated with immunodeficiency syndrome whereas overexpression or

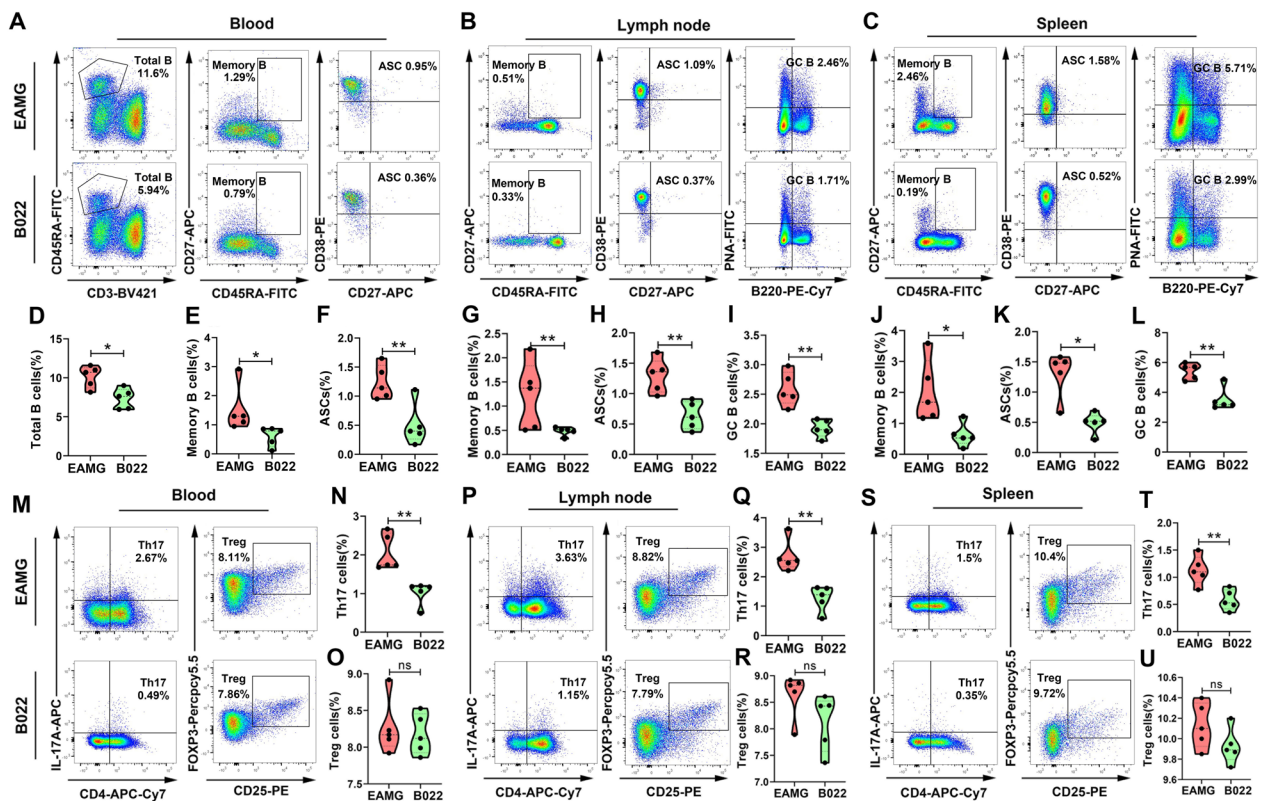


Fig.8 B022 alters the frequency of EAMG rat B and CD4⁺T cell subsets in vivo. **A–C** The dot plots represent flow gating diagram of B cell subsets (total B, memory B, ASCs and GC B cells). **D–L** The percentage of total B, memory B, ASCs and GC B cells between EAMG (n = 5) and B022 group (n = 5) in blood, lymph node and spleen. (M,P,S) The dot plots represent flow gating diagram of T cell subsets (Th17 and Treg cells). **D–L** The percentage of Th17 and Treg cells between EAMG (n = 5) and B022 group (n = 5) in blood, lymph node and spleen. Data are displayed as means ± SD. Statistical analysis was conducted by independent sample t-test (*P < 0.05, **P < 0.01, ***P < 0.001, ns: non-significant)

overactivation of NIK is observed in various autoimmune diseases or malignancies [25]. Our study also found that NIK expression was elevated on B cells and CD4⁺T cells in MG patients. Notably, the expression level of NIK in the serum of MG patients was also increased, which was related to the disease severity and disease state, suggesting that serum NIK may be a potential biomarker to monitor the condition of patients. Subgroup analysis revealed that NIK levels were increased in GMG patients than in OMG, as well as elevated in TAMG than in non-TAMG. Here, we noted that most TAMG patients belonged to the GMG category, which may explain the high expression of NIK in TAMG patients.

As a protein kinase, NIK primarily regulates its activity by inducing its degradation at the protein level, without requiring phosphorylation [28]. For this reason, studies in drug discovery focused on specific novel small molecule inhibitors to curb the activity of NIK. Small molecule kinase inhibitors usually have significant advantages over biologics due to their broad efficacy, convenience, and tissue penetration [29]. In the treatment of autoimmune

diseases associated with non-classical NF-κB signaling pathway activation, such as systemic lupus erythematosus, rheumatoid arthritis, inflammatory bowel disease, multiple sclerosis and ANCA-associated vasculitis (AAV), the inhibition of NIK has been demonstrated to possess potential therapeutic value [12, 13, 30–32]. The employment of the NIK inhibitor manifested that NIK kinase activity assumes a positive function in regulating multiple crucial pathways, such as BAFF, OX40, CD40, ICOS, IL-21, and TNFRSF12A signaling or downstream p100-to-p52 processing. Additionally, the inhibition of this activity exhibited protective consequences in pre-clinical lupus, periodontitis, liver inflammation or amyotrophic lateral sclerosis models [13, 33–35]. Next, we investigated for the first time the effects of novel NIK inhibitor B022 on pathogenic immune cells in our culture system. Our study found that B022 prominently inhibited B cell activation, proliferation and ASCs differentiation, which was consistent with the previous effect of another NIK inhibitor, SIM1, on B cells in AAV patients [12]. Moreover, NIK has also been reported to play an essential

T cell-intrinsic role, regulating TCR signaling and influencing T cell activation and differentiation [27, 36]. In our PBMC culture system, we also observed that B022 effectively inhibited the activation and differentiation of CD4⁺T cells, without impacting the T cell count, proliferation, or apoptosis. These results suggest that NIK has a remodeling effect on MG immune microenvironment.

Apart from generating antibodies, B cells also have the function of antigen presentation and cytokine production [37]. Then, we comprehensively assessed the effect of NIK inhibitor B022 on B cell function in B cell culture system, and confirmed for the first time that B022 can downregulate the expression of B cell antigen-presenting markers CD80, CD86, and CD95, as well as pro-inflammatory cytokines IL-6 and GM-CSF. At the same time, ASCs (plasmablasts and plasma cells) differentiation and antibody titers were also impaired in cultures with B022 inhibitor, especially transcription factors regulating the differentiation of mature B cells into plasma cells were significantly affected. These results generated from our in vitro experiment supported the fact that NIK inhibitor B022 effectively shapes B-cell homeostasis without causing persistent B-cell depletion (e.g. as observed upon treatment with CD20 monoclonal antibody). To observe the therapeutic effect of NIK small molecule kinase inhibitors on MG, in vivo experiment was carried out. It was observed that B022 treatment ameliorated the severity of EAMG rats, reduced proportion of pathogenic B and T cell subsets, anti-AchR antibody levels and postsynaptic membrane damage. In summary, we can see from in vitro and in vivo experiments that NIK inhibitor B022 has the following advantages over CD20 monoclonal antibody such as rituximab. First, B cells undergo phenotypic changes during maturation. CD20 is expressed in pre-B cells to memory B cells, but is not found in plasmablasts or plasma cells (PCs). In principle, both plasmablasts and PCs can produce antibodies, but are not targets for anti-CD20 antibodies. This treatment gap has been demonstrated in MG patients who have not responded adequately to previous anti-CD20 therapy. Our study found that NIK inhibitor B022 can effectively inhibit the differentiation of B cells into plasmablasts and PCs, and reduce IgG and IgM antibody levels in vitro. In vivo experiments, it was also found that the decline of ASCs was accompanied by the downregulation of anti-AchR antibody, which fully indicated that B022 could affect the differentiation and function of ASCs. Second, monoclonal antibodies often require repeated dosing, because even if effective, the benefits tend to be short-lived. One reason for the limited efficacy is the lack of depth of depletion. While circulating B cells can be efficiently cleared by antibodies, the same is not true of B cells in inflammatory niches, such as those in neuromuscular synapses, spleen,

lymph nodes, or bone marrow [38]. However, our study found that B022 reduced total B cells and the proportion of GC-B and ASCs cells in spleen and lymph nodes, with increased AchR clusters in neuromuscular junctions and down-regulated complement deposition. Third, CD20 monoclonal antibodies usually rely on passive diffusion into tissues and also require the activity of other components to play a B-cell deletion role. Natural killer cells (NK) and/or macrophages are required for antibody-dependent cytotoxicity (ADCC) and antibody-dependent phagocytosis (ADPC), while complement factors are required for complement dependent cytotoxicity (CDC). In autoimmune diseases, both NK cells and macrophages may be impaired in function. For example, NK cells in MG exhibit impaired cytotoxic function [39]. MG is also classified as a complement disease, in which the depletion of complement may limit the availability of CDC complement [40]. However, NIK inhibitors exhibit direct immunomodulatory effects on pathogenic B and T cells, potentially offering significant advantages. Moreover, while rituximab effectively depletes peripheral B cells, this action also heightens the risk of infection. Although B022 mitigates the disease-causing functions of B cells, it preserves a portion of these cells, thereby avoiding complete disruption of humoral immunity. All the mentioned above provides very important preclinical evidence for the future use of NIK inhibitors in the clinic.

Our study has some limitations. Firstly, the EAMG rat model is a classic model for studying antibody production against the neuromuscular junction and neuromuscular transmission impairment. However, it does not fully replicate the human pathology, as the disease is induced through forced sensitization to the antigen. Although preclinical animal models represent a required step to justify and support clinical trials, subtle differences in the immune systems of EAMG rat model and human pathology might have to be taken into account. Secondly,

this was a single-center study and the number of patients included was relatively low. The clinical heterogeneity of MG patients is large, which may lead to some differences in the data distribution in this study. In the future, we plan to expand the sample size and conduct multi-center studies to observe the role of NIK in MG. Thirdly, despite satisfactory results of NIK inhibitors at the cellular level in vitro and in preclinical animal studies, but NIK is expressed in both adaptive and innate immune cells, and the use of NIK inhibitors may lead to non-selective suppression of immune cells (e.g., a decrease in the proportion of NK and Treg cells), which also requires more caution in clinical application. Fourthly, our in vivo experiment did not set up drug concentration gradient administration, and different doses of B022 inhibitors can be administered in the future to investigate the

dose–effect relationship of the drug and verify the efficacy and safety of the drug, thereby adding more preclinical evidence for future clinical trials.

Conclusions

In conclusion, we describe a hallmark gene on the NF- κ B and TNF signaling pathways, namely NIK, which is conspicuously upregulated in the B cells of MG patients, and serum NIK levels can serve as a novel biomarker to monitor the progression of the disease. Another important finding is that targeting NIK with small molecule kinase inhibitors can effectively shape B cell homeostasis, and exhibited protective consequences in EAMG rat model. Collectively, targeting NIK may be an effective novel treatment strategy for MG.

Abbreviations

AAV	ANCA-associated vasculitis
AchR	Acetylcholine receptor
ASCs	Antibody-secreting cells
BCDT	B cell depleting therapy
CCK8	Cell Counting Kit-8
EAMG	Experimental autoimmune MG
ELISA	Enzyme-linked immunosorbent assay
HCs	Healthy controls
HE	Hematoxylin–Eosin
MG	Myasthenia gravis
NMJ	Neuromuscular junction
RT-qPCR	Real-time quantitative PCR
RTX	Rituximab

Supplementary Information

The online version contains supplementary material available at <https://doi.org/10.1186/s12974-025-03342-5>.

Supplementary material 1.

Supplementary material 2.

Acknowledgements

We thank the patients who agreed to participate in this study as well as the doctors and nurses from the Department of Neurology, Affiliated Hospital of Xuzhou Medical University who participated in this study.

Author contributions

XYH, ZAZ and ZYW were involved in conception and design of the study, acquisition and analysis of data and drafting or revising a significant portion of the manuscript or figures. TCL, MJY, XYG, XD and TYM were involved in acquisition and analysis of data. YZ was involved in drafting or revising a significant portion of the manuscript or figures.

Funding

This work was supported by The Open Project of Key Laboratory of Colleges and Universities in Jiangsu Province (XZSYSKF2021041), Science and Technology Development Fund of Affiliated Hospital of Xuzhou Medical University (XYFM2021017), Medical research project of Jiangsu Provincial Health Commission (M2022118), Xuzhou Health and Health Commission Youth Innovation Science and Technology Project (XWKYHT20240110), The Natural Science Foundation of Jiangsu Province (BK20231158).

Data availability

The data sets used and/or analyzed during this study are available from the corresponding author on reasonable request.

Declarations

Ethics approval and consent to participate

The Ethics Committee of the Affiliated Hospital of Xuzhou Medical University granted approval for this study (XYFY2023-KL471-01), and all participants provided written informed consent. All the animal experimental protocols were approved by the Ethics Committee of Xuzhou Medical University (202410T016).

Consent for publication

Not applicable.

Competing interests

The authors declare no competing interests.

Received: 14 November 2024 Accepted: 10 January 2025

Published online: 24 January 2025

References

- Gilhus NE. Myasthenia gravis. *N Engl J Med*. 2016;375:2570–81.
- Melzer N, Ruck T, Fuhr P, Gold R, Hohlfeld R, Marx A, Melms A, Tackenberg B, Schälke B, Schneider-Gold C, et al. Clinical features, pathogenesis, and treatment of myasthenia gravis: a supplement to the Guidelines of the German neurological society. *J Neurol*. 2016;263:1473–94.
- Uzawa A, Utsugisawa K. Biological therapies for myasthenia gravis. *Expert Opin Biol Ther*. 2023;23:253–60.
- Dalakas MC. Immunotherapy in myasthenia gravis in the era of biologics. *Nat Rev Neurol*. 2019;15:113–24.
- Piehl F, Eriksson-Dufva A, Budzianowska A, Feresiadou A, Hansson W, Hietala MA, Håkansson I, Johansson R, Jons D, Kmezcic I, et al. Efficacy and safety of rituximab for new-onset generalized myasthenia gravis: the RINOMAX randomized clinical trial. *JAMA Neurol*. 2022;79:1105–12.
- Sahai SK, Maghzi AH, Lewis RA. Rituximab in late-onset myasthenia gravis is safe and effective. *Muscle Nerve*. 2020;62:377–80.
- Nowak RJ, Coffey CS, Goldstein JM, Dimachkie MM, Benatar M, Kissel JT, Wolfe GI, Burns TM, Freimer ML, Nations S, et al. Phase 2 trial of rituximab in acetylcholine receptor antibody-positive generalized myasthenia gravis: the BeatMG study. *Neurology*. 2022;98:e376–e389.
- Dos Santos A, Noury JB, Genestet S, Nadaj-Pakleza A, Cassereau J, Baron C, Videt D, Michel L, Pereon Y, Wiertelowski S, et al. Efficacy and safety of rituximab in myasthenia gravis: a French multicentre real-life study. *Eur J Neurol*. 2020;27:2277–85.
- Brauner S, Eriksson-Dufva A, Hietala MA, Frisell T, Press R, Piehl F. Comparison between rituximab treatment for new-onset generalized myasthenia gravis and refractory generalized myasthenia gravis. *JAMA Neurol*. 2020;77:974–81.
- Ruetsch-Chelli C, Bresch S, Seitz-Polski B, Rosenthal A, Desnuelle C, Cohen M, Brglez V, Ticchioni M, Lebrun-Frenay C. Memory B cells predict relapse in rituximab-treated myasthenia gravis. *Neurotherapeutics*. 2021;18:938–48.
- Ramírez-Valle F, Maranville JC, Roy S, Plenge RM. Sequential immunotherapy: towards cures for autoimmunity. *Nat Rev Drug Discov*. 2024;23:501–24.
- Merino-Vico A, van Hamburg JP, Tuijnburg P, Frazzei G, Al-Soudi A, Bonasia CG, Helder B, Rutgers A, Abdulhad WH, Stegeman CA, et al. Targeting NF- κ B signaling in B cells as a potential new treatment modality for ANCA-associated vasculitis. *J Autoimmun*. 2024;142: 103133.
- Brightbill HD, Suto E, Blaquiére N, Ramamoorthi N, Sujatha-Bhaskar S, Gogol EB, Castaneda GM, Jackson BT, Kwon YC, Haller S, et al. NF- κ B inducing kinase is a therapeutic target for systemic lupus erythematosus. *Nat Commun*. 2018;9:179.
- Li MY, Chong LC, Duns G, Lytle A, Woolcock B, Jiang A, Telenius A, Ben-Neriah S, Nawaz W, Slack GW, et al. TRAF3 loss-of-function reveals the noncanonical NF- κ B pathway as a therapeutic target in diffuse large B cell lymphoma. *Proc Natl Acad Sci USA*. 2024;121: e2320421121.
- Decombis S, Papin A, Bellanger C, Sortais C, Dousset C, Le Bris Y, Riveron T, Blandin S, Hulin P, Tessoulin B, et al. The IL32/BAFF axis supports

- prosurvival dialogs in the lymphoma ecosystem and is disrupted by NIK inhibition. *Haematologica*. 2022;107:2905–17.
16. Brightbill HD, Jackman JK, Suto E, Kennedy H, Jones C 3rd, Chalasani S, Lin Z, Tam L, Roose-Girma M, Balazs M, et al. Conditional deletion of NF- κ B-inducing kinase (NIK) in adult mice disrupts mature B cell survival and activation. *J Immunol*. 2015;195:953–64.
 17. Hahn M, Macht A, Waisman A, Hövelmeyer N. NF- κ B-inducing kinase is essential for B-cell maintenance in mice. *Eur J Immunol*. 2016;46:732–41.
 18. Willmann KL, Klaver S, Doğu F, Santos-Valente E, Garncarz W, Bilic I, Mace E, Salzer E, Conde CD, Sic H, et al. Biallelic loss-of-function mutation in NIK causes a primary immunodeficiency with multifaceted aberrant lymphoid immunity. *Nat Commun*. 2014;5:5360.
 19. Sanders DB, Wolfe GI, Benatar M, Evoli A, Gilhus NE, Illa I, Kuntz N, Massey JM, Melms A, Murai H, et al. International consensus guidance for management of myasthenia gravis: executive summary. *Neurology*. 2016;87:419–25.
 20. Huang X, An X, Gao X, Wang N, Liu J, Zhang Y, Qi G, Zhang C. Serum amyloid A facilitates expansion of CD4⁺ T cell and CD19⁺ B cell subsets implicated in the severity of myasthenia gravis patients. *J Neurochem*. 2024;168:224–37.
 21. Marken J, Muralidharan S, Giltiy NV. Anti-CD40 antibody KPL-404 inhibits T cell-mediated activation of B cells from healthy donors and autoimmune patients. *Arthritis Res Ther*. 2021;23(1):5.
 22. Yang CL, Zhang P, Liu RT, Zhang N, Zhang M, Li H, Du T, Li XL, Dou YC, Duan RS. CXCR5-negative natural killer cells ameliorate experimental autoimmune myasthenia gravis by suppressing follicular helper T cells. *J Neuroinflamm*. 2019;16:282.
 23. Gilhus NE, Skeie GO, Romi F, Lazaridis K, Zisimopoulou P, Tzartos S. Myasthenia gravis—autoantibody characteristics and their implications for therapy. *Nat Rev Neurol*. 2016;12:259–68.
 24. Chen X, Qiu J, Gao Z, Liu B, Zhang C, Yu W, Yang J, Shen Y, Qi L, Yao X, et al. Myasthenia gravis: molecular mechanisms and promising therapeutic strategies. *Biochem Pharmacol*. 2023;218: 115872.
 25. Pflug KM, Sitcheran R. Targeting NF- κ B-inducing kinase (NIK) in immunity, inflammation, and cancer. *Int J Mol Sci*. 2020;21:8470.
 26. Haselager MV, Eldering E. The therapeutic potential of targeting NIK in B cell malignancies. *Front Immunol*. 2022;13: 930986.
 27. Lacher SM, Thurm C, Distler U, Mohebiany AN, Israel N, Kitic M, Ebering A, Tang Y, Klein M, Wabnitz GH, et al. NF- κ B inducing kinase (NIK) is an essential post-transcriptional regulator of T-cell activation affecting F-actin dynamics and TCR signaling. *J Autoimmun*. 2018;94:110–21.
 28. Tao Z, Ghosh G. Understanding NIK regulation from its structure. *Structure*. 2012;20:1615–7.
 29. Zarrin AA, Bao K, Lupardus P, Vucic D. Kinase inhibition in autoimmunity and inflammation. *Nat Rev Drug Discov*. 2021;20:39–63.
 30. Aya K, Alhawagri M, Hagen-Stapleton A, Kitaura H, Kanagawa O, Novack DV. NF-(κ)B-inducing kinase controls lymphocyte and osteoclast activities in inflammatory arthritis. *J Clin Invest*. 2005;115:1848–54.
 31. Nguyen VQ, Eden K, Morrison HA, Sammons MB, Knight KK, Sorrentino S, Brock RM, Grider DJ, Allen IC, Sorrentino D. Noncanonical NF- κ B signaling upregulation in inflammatory bowel disease patients is associated with loss of response to anti-TNF agents. *Front Pharmacol*. 2021;12: 655887.
 32. Jin W, Zhou XF, Yu J, Cheng X, Sun SC. Regulation of Th17 cell differentiation and EAE induction by MAP3K NIK. *Blood*. 2009;113:6603–10.
 33. Wang J, Wang B, Lv X, Wang L. NIK inhibitor impairs chronic periodontitis via suppressing non-canonical NF- κ B and osteoclastogenesis. *Pathog Dis*. 2020;78:ftaa045.
 34. Ren X, Li X, Jia L, Chen D, Hou H, Rui L, Zhao Y, Chen Z. A small-molecule inhibitor of NF- κ B-inducing kinase (NIK) protects liver from toxin-induced inflammation, oxidative stress, and injury. *FASEB J*. 2017;31:711–8.
 35. Cao M, Yi L, Xu Y, Tian Y, Li Z, Bi Y, Guo M, Li Y, Liu Y, Xu X, et al. Inhibiting NF- κ B inducing kinase improved the motor performance of ALS animal model. *Brain Res*. 2024;1843: 149124.
 36. Li Y, Wang H, Zhou X, Xie X, Chen X, Jie Z, Zou Q, Hu H, Zhu L, Cheng X, et al. Cell intrinsic role of NF- κ B-inducing kinase in regulating T cell-mediated immune and autoimmune responses. *Sci Rep*. 2016;6:22115.
 37. Rastogi I, Jeon D, Moseman JE, Muralidhar A, Potluri HK, McNeel DG. Role of B cells as antigen presenting cells. *Front Immunol*. 2022;13: 954936.
 38. Chen TX, Fan YT, Peng BW. Distinct mechanisms underlying therapeutic potentials of CD20 in neurological and neuromuscular disease. *Pharmacol Ther*. 2022;238: 108180.
 39. Zhang Q, Han X, Bi Z, Yang M, Lin J, Li Z, Zhang M, Bu B. Exhausted signature and regulatory network of NK cells in myasthenia gravis. *Front Immunol*. 2024;15:1397916.
 40. Howard JF Jr. Myasthenia gravis: the role of complement at the neuromuscular junction. *Ann NY Acad Sci*. 2018;1412(1):113–28.

Publisher's Note

Springer Nature remains neutral with regard to jurisdictional claims in published maps and institutional affiliations.